Chemical Engineering Journal 361 (2019) 929–936

Contents lists available at ScienceDirect

Chemical Engineering Journal

journal homepage: www.elsevier.com/locate/cej

Degradation of the flame retardant triphenyl phosphate by ferrous ion-activated hydrogen peroxide and persulfate: Kinetics, pathways, and mechanisms

Qingyun Song, Yiping Feng*, Guoguang Liu, Wenying Lv

Guangzhou Key Laboratory Environmental Catalysis and Pollution Control, Guangdong Key Laboratory of Environmental Catalysis and Health Risk Control, School of Environmental Science and Engineering, Institute of Environmental Health and Pollution Control, Guangdong University of Technology, Guangzhou 510006, China

HIGHLIGHTS

- Both Fenton and Fe^{2+}/PS processes are efficient for TPhP degradation from water.
- Natural water matrix significantly affected TPhP degradation.
- HO· and SO4·$^{-}$ are predominant radicals in Fenton and Fe^{2+}/PS process, respectively.
- Similar intermediates of TPhP in both processes were identified using LC-MS.

ARTICLE INFO

Keywords:
Triphenyl phosphate
Hydroxyl radical
Sulfate radical
Degradation products

ABSTRACT

The efficacies of ferrous ion-activated hydrogen peroxide (Fe^{2+}/H_2O_2, Fenton) and persulfate ($Fe^{2+}/S_2O_8^{2-}$, Fe^{2+}/PS) processes for degrading triphenyl phosphate (TPhP) in aqueous solutions were systemically investigated and compared. Both Fenton and Fe^{2+}/PS processes can effectively degrade TPhP in water. A fast TPhP degradation was achieved in 5 min by Fenton oxidation, while TPhP was gradually degraded with prolonging reaction time via Fe^{2+}/PS oxidation. The effects of operating parameters, including oxidant and Fe^{2+} dosage, pH, and water constitutes, on TPhP degradation were systemically evaluated. TPhP removal was increased as the oxidant and Fe^{2+} dosage increase, while TPhP degradation was not greatly changed under the examined pH (4.0–9.0). Water constitutes, humic acid, and anions (Cl^- and NO_3^-) did not obviously influence TPhP degradation for both processes. However, HCO_3^- significantly inhibited TPhP oxidation, and the inhibition was inversely related to HCO_3^- concentrations. Radical quenching experiments and electron paramagnetic resonance spectrometry revealed that HO· was the dominant radical in Fenton process whereas SO4·$^{-}$ played a dominant role in Fe^{2+}/PS process for TPhP degradation. Moreover, TPhP removal in various natural water matrices was examined to better understand the feasibility of AOPs on the elimination of TPhP from natural waters. The lower removal of TPhP indicates that both of high oxidant dosage and/or long reaction time were required to achieve high removal efficiency and high mineralization. Furthermore, TPhP degradation products were identified through LC-MS/MS technology. Similar products were observed in both oxidation processes, and the degradation pathways mainly involved hydroxylation and phenoxy bond cleavage. The results of this study indicates that it is technically feasible for applying HO· and SO_4·$^{-}$ based AOPs to treat TPhP contamination in water/wastewater.

1. Introduction

Due to the phase-out of some brominated flame retardants (BFRs), the use of organophosphate flame retardants (OPFRs) as the alternative flame retardants has been increasingly adopted recently [1]. OPFRs have been detected widely in air and dust [2], water [3], sediment [4], and biota [5]. Triphenyl phosphate (TPhP) is a high production volume OPFRs that has been detected in multiple environmental media with increasing concentrations these years [2,6]. The environmental and health risks of TPhP have drawn attention because of its potential multiplex toxicities (e.g., neurotoxicity and developmental toxicity) to organisms [7,8]. Therefore, it is necessary to develop a cost-effective

* Corresponding author.
E-mail address: ypfeng@gdut.edu.cn (Y. Feng).

https://doi.org/10.1016/j.cej.2018.12.140
Received 18 August 2018; Received in revised form 23 December 2018; Accepted 24 December 2018
Available online 26 December 2018
1385-8947/

and environmental-friendly treatment methods to remove such OPFRs from their contaminated water.

Advanced oxidation processes (AOPs), with the highly reactive hydroxyl radical (HO·) or sulfate radical ($SO_4\cdot^-$) as the main oxidative species, are promising for eliminating organic pollutants in aquatic environment [9,10]. Both HO· and $SO_4\cdot^-$ are powerful oxidants for the degradation of the organic contaminants due to their high standard reduction potentials, i.e., HO· (E^0 = 1.9–2.7 V) and $SO_4\cdot^-$ (E^0 = 2.5–3.1 V) [11]. Because of their strong oxidation ability and cost-effectiveness, both HO· and $SO_4\cdot^-$ based AOPs have been considered as the promising *in situ* chemical oxidation (ISCO) technologies for remediating contaminated water and wastewater [12]. Fenton reaction, hydrogen peroxide (H_2O_2) activated by ferrous ion (Fe^{2+}) that could generate HO·, has been widely used for remediating soil and groundwater [13,14]. The mechanism of Fenton reaction mainly includes a series of chain and radical reactions, as described in Eqs. ((1)–(6)) [15,16]. Fenton reaction prefers acidic pH [16], which greatly limited its practical application for water treatment at neutral and basic conditions

$$H_2O_2 + Fe^{2+} \rightarrow HO^{\cdot} + HO^- + Fe^{3+} \quad (1)$$

$$H_2O_2 + Fe^{3+} \rightarrow HO_2^{\cdot} + HO^+ + Fe^{2+} \quad (2)$$

$$HO^{\cdot} + H_2O_2 \rightarrow HO_2^{\cdot} + H_2O \quad (3)$$

$$HO_2^{\cdot} \rightarrow O_2^{\cdot-} + H^+ \quad (4)$$

$$HO_2^{\cdot} + Fe^{2+} + H^+ \rightarrow H_2O_2 + Fe^{3+} \quad (5)$$

$$HO^{\cdot} + Fe^{2+} \rightarrow HO^- + Fe^{3+} \quad (6)$$

Recently, persulfate ($S_2O_8^{2-}$, PS), a popular ISCO oxidant, has received increasing attention in environmental applications due to its several advantages. $SO_4\cdot^-$ can be formed by activating PS via various approaches, including heat [17], UV [18], transit-metal cations or metal oxides [19–22], base, and carbon nanomaterials [23]. Compared to HO·, $SO_4\cdot^-$ is more stable and selective because $SO_4\cdot^-$ mainly reacts with organic compounds through electron transfer mechanism [24]. Previous studies have found that the consumption of $SO_4\cdot^-$ by non-target water constituents, such as natural organic matters, is much slower than that of HO·, indicating that $SO_4\cdot^-$ based AOPs may be more efficient than HO· when they are used for natural water remediation [25,26]. Fe^{2+} is the most frequently used metal ion for PS activation [27,28]. Similar to Fenton reaction, the mechanism of Fe^{2+} activated PS (Fe^{2+}/PS) process is shown in Eqs. ((7)–(9)). However, the excess Fe^{2+} could scavenge $SO_4\cdot^-$ through Eq. (8), so the oxidation efficiency of target contaminants would be greatly reduced. Therefore, it is vital to confirm the proper dosages of Fe^{2+} and PS during the contaminant treatment.

$$S_2O_8^{2-} + Fe^{2+} \rightarrow Fe^{3+} + SO_4^{2-} + SO_4^{\cdot-} \quad (7)$$

$$SO_4^{\cdot-} + Fe^{2+} \rightarrow Fe^{3+} + SO_4^{2-} \quad (8)$$

$$SO_4^{\cdot-} + S_2O_8^{2-} \rightarrow SO_4^{2-} + S_2O_8^{\cdot-} \quad (9)$$

To date, exploration on the potential application of AOPs for the treatment of OPFRs is still in its early stage. The processes, including photocatalysis [29–32], UV [33], UV/H_2O_2 [34–36], UV/O_3 [37], UV/peroxymonosulfate, and UV/persulfate [38,39], have been used for eliminating OPFRs from water. Pseudo-first order kinetics of OPFRs degradation was confirmed [29–31,33–35], and these OPFRs were transformed into hydroxylated products through both of radical addition and C-O bond cleavage routes [31,32,36,38,39]. OPFRs degradation in natural water or wastewater matrix was significantly reduced [30,31,38]. However, few efforts have been devoted to the degradation process (i.e., degradation kinetics, products, and mechanisms) for TPhP, one of aromatic OPFRs. Yuan et al. [40] demonstrated that TPhP at 50 μg L^{-1} could be quickly degraded through ozone and UV/H_2O_2 processes, and 96% TPhP was removed via ozone and 100% TPhP was removed via UV/H_2O_2 after 30 min treatment, respectively. Yu et al. [41] simulated the TPhP degradation process which was initiated by HO· through quantum chemistry calculations, and found that the reaction rate constant was 1.6 × 10^{-12} cm^3 $molecule^{-1}$ s^{-1} at 298 K with TPhP-OH adduct and phenol phosphate as the main degradation products. Li et al. [42] also found that TPhP was rapidly degraded by HO· with the reaction rate constant around 8 × 10^9 M^{-1} s^{-1}. Nevertheless, to the best of our knowledge, no information is available on the oxidation of TPhP through $SO_4\cdot^-$ based AOPs. In addition, HO· initiated TPhP degradation process needs to be systematically examined, including the degradation kinetics and degradation products.

In this study, the degradation processes of TPhP by Fenton and Fe^{2+}/PS reactions were systematically investigated, respectively. A series of kinetic experiments were conducted to explore the effects of Fe^{2+} and oxidant (i.e, H_2O_2 and PS) dosages, respectively. In natural water, pHs varied and inorganic anions, as well as natural organic matter (NOM) are ubiquitously present, which can potentially influence the AOPs [43,44]. Therefore, the effects of pH, humic acid (HA), and inorganic anions (e.g., Cl^-, NO_3^-, and HCO_3^-) on the degradation of TPhP were also investigated in this study, respectively. TPhP degradation intermediates were identified through liquid chromatography-tandem mass spectrometry (LC–MS) and the detailed degradation mechanisms and transformation pathways were proposed. Especially, the TPhP degradation efficiency in different natural waters was examined to evaluate the technical feasibility of both Fenton and Fe^{2+}/PS processes on the treatment of TPhP from water/wastewater.

2. Materials and methods

2.1. Chemicals and materials

All chemicals were commercially available with highest purity and directly used without further purification. Triphenyl phosphate (TPhP, ≥99%) was purchased from Sigma-Aldrich (St. Louis, MO, USA). Ferrous sulphate heptahydrate ($FeSO_4{\cdot}7H_2O$, 98%) was obtained from Damao Chemical Reagent Co. (Tianjin, China). Hydrogen peroxide (H_2O_2, 30.0%) was obtained from Sinopharm Chemical Reagent Co., Ltd (Shanghai, China). Potassium persulfate ($K_2S_2O_8$, 99.5%) and humic acid (HA, 90%) were obtained from Aladdin Chemistry Co. Ltd (Shanghai, China). Acetonitrile, methanol, and formic acid of HPLC grade were purchased from TEDIA (Fairfield, USA). Ethanol (EtOH) and tertiary butanol (TBA) in analytical grade were obtained from Guangzhou Chemical Reagent Factory (Guangzhou, China). Deionized (DI) water (> 18 mΩ·cm, Milli-Q system) was used for solution preparation. The stock solution (10 mM) of TPhP was prepared in HPLC grade acetonitrile and stored at 4 °C for further use.

2.2. Experimental procedure

To avoid any interference related to potential side reactions between hydroxyl and sulfate radicals with buffer species (i.e., PO_4^{3-}, CO_3^{2-}), the experiments were performed without any buffer solutions. Without specified, all the reactions were performed in 30 mL brown glass test vials sealed with Teflon-lined silicone septa at 25.0 ± 0.2 °C. 10 μM of TPhP solution and certain volume of H_2O_2/PS were firstly introduced to the vial. 0.01 M H_2SO_4 or NaOH was used to adjust solution pH, and no further pH adjustment was performed during the degradation process. Following that, the desired dosage of ferrous ion (Fe^{2+}) was employed to initiate the reaction. At the defined time intervals, 1.0 mL of aqueous sample was withdrawn and immediately quenched by 1.0 mL pure methanol. After filtered by a 0.45 μm membrane filter (Anpel, Shanghai, China), the residual TPhP was quantified for further analysis.

The influence of Fe^{2+} concentrations (0–500 μM) and H_2O_2/PS dosages (0–1000 μM) on TPhP degradation were evaluated at pH 4.0,

respectively. The effect of pH on TPhP degradation via both Fe^{2+}/H_2O_2 and Fe^{2+}/PS oxidation systems was examined at 25 °C with pH values from 4.0 to 9.0. Solution pH was adjusted before the addition of Fe^{2+} to avoid the interference of Fe^{2+} oxidation. The effects of typical natural water constituents on TPhP oxidation, including various inorganic anions (i.e., Cl^-, NO_3^-, and HCO_3^-) and HA, a representative dissolved organic matter, were also investigated. All experiments were conducted in triplicate, and the mean values were reported.

Natural water samples, including sea water collected from South China Sea in Huizhou, municipal wastewater effluent obtained from an activated sludge sewage treatment plant (STP) in Guangzhou, river water collected from the Pearl River in Guangzhou, and tap water obtained from pipeline in our laboratory were also used in this study to investigate the oxidation efficiency of TPhP in natural waters. The collected water samples were taken to the laboratory within 12 h and stored at 4 °C for further use. Prior to use, all collected waters were filtered through a 0.45 μm membrane filter (Anpel, Shanghai, China) to remove particulate matters. The corresponding physicochemical parameters of the water samples were characterized and listed in Table S1 in Supplementary Materials.

2.3. Identification of hydroxyl and sulfate radicals

Radical scavengers were applied to identify the radicals formed during the Fenton and Fe^{2+}/PS oxidation processes. To differentiate the role of HO· and $SO_4\cdot^-$ radicals in TPhP degradation process, the excessive amount of EtOH and t-BuOH were initially added into the reaction solutions as the scavengers at 12.5 mM, respectively. The reaction conditions were kept identical throughout the experiments.

5, 5-dimethyl-1-pyrroline N-oxide (DMPO) was applied to capture HO· and $SO_4\cdot^-$ radicals *in situ*, which were produced from Fenton and Fe^{2+}/PS processes. Once the reaction was initiated, 20 μL of 100 mM DMPO solution was spiked into 180 μL of reaction solution within 5 s and shaken for 2 min. Then, the spectra of radical adducts were recorded using an electron paramagnetic resonance spectrometer (EPR, EMXPlus-10/12, Bruker, Germany).

2.4. Identification of TPhP transformation products

The same reaction systems, including TPhP/Fe^{2+}/H_2O_2 and TPhP/Fe^{2+}/PS as described above in Section 2.2. *Experimental procedure*, were used for TPhP degradation transformation product identification. After passing through the 0.45 μm membrane filter (Anpel, Shanghai, China), each sample was concentrated by an Oasis HLB cartridge (6 mL, 500 mg, Waters) through solid-phase extraction (SPE) process following the procedure described in our previous studies [45,46]. In brief, the cartridge was firstly activated by 10 mL pure methanol and 10 mL DI water, consequently. Then the reaction sample was passed through the cartridge at a flow rate at 5 mL min^{-1}. Finally, the extracts were eluted with 2 × 2 mL methanol, and then dried with a gentle nitrogen flow. The obtained products were finally re-dissolved with 1 mL methanol and then analyzed by HPLC-MS/MS.

2.5. Analytical methods

The concentration of the residual TPhP was analyzed through a Waters alliance e2695 high performance liquid chromatograph (HPLC, Waters, USA) equipped with a diode array detector and a Waters XBridge C18 reversed-phase column (4.6 × 250 mm, 5 μm). The mobile phase was made up of 65% acetonitrile and 35% DI water, with elution rate at 1 mL min^{-1}. The injection volume was 20 μL. The column temperature was set up at 35 °C, and the detection wavelength was set as 210 nm.

HPLC-MS/MS analysis was carried out on an Agilent 1200 series HPLC connected to a G6410B triple quadrupole mass spectrometer (Agilent Technologies, USA) through an ESI interface. Separation was performed on a C18 reverse-phase column (4.6 × 150 mm, 5 μm, Agilent). Injection volume was set as 10 μL. Elution was performed at a flow rate of 0.2 mL min^{-1} with H_2O as eluent A and methanol as eluent B. The mass spectrometer was operated in positive ionization mode over the range m/z = 100–1000. Capillary exit and skimmer voltages was 113.5 V and 40 V, respectively. Dry temperature was 350 °C. Nitrogen was used as dry gas at a flow rate of 10 L min^{-1} and as collision gas with 99.99% purity. Nebulizer pressure was 40 psi.

The phosphate ion (PO_4^{3-}) in the reaction solutions was measured with Mo-Sb Anti-spectrophotometer method with a minimum detection limit 0.005 mg L^{-1}. Total organic carbon (TOC) content was determined by a TOC analyzer (Shimadzu, TOC-L CPH, Japan).

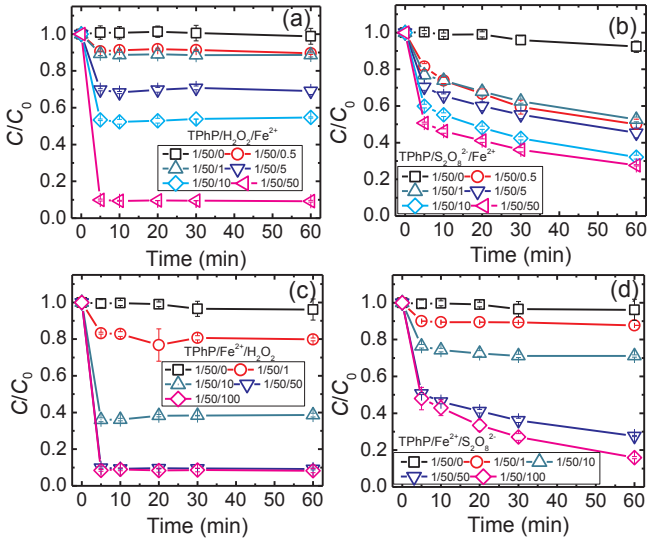

Fig. 1. Effect of ferrous ion concentration (a, b) and oxidant dosage (c, d) on TPhP degradation by (a, c) Fenton process and (b, d) Fe^{2+}/PS process. Experimental conditions: $[TPhP]_0$ = 10 μM, $pH_{initial}$ = 4.0, T = 25 °C. $[H_2O_2]_0$ = $[PS]_0$ = 500 μM, $[Fe^{2+}]_0$ = 0–500 μM in (a, b), and $[Fe^{2+}]_0$ = 500 μM, $[H_2O_2]_0$ = $[PS]_0$ = 0–1000 μM in (c, d). Errors represent the standard deviation (n = 3).

3. Results and discussion

3.1. Degradation kinetics of TPhP in DI water

3.1.1. Effect of Fe^{2+} dosage

As shown in Fig. 1a and b, the degradation of TPhP was negligible by direct H_2O_2 (< 2%) and $S_2O_8^{2-}$ (PS, < 8%) oxidation after 60 min reaction, indicating that only H_2O_2 or PS was not sufficient to oxidize TPhP due to its stable structure. However, TPhP degradation was obviously accelerated by ferrous ion (Fe^{2+}) activation of both oxidants. It is well known that HO· is generated in Fenton process [13], and $SO_4\cdot^-$ is produced in PS activation process [12]. More HO· and $SO_4\cdot^-$ were generated with increasing Fe^{2+} dosage, thus resulting in an enhanced degradation efficacy of TPhP. With a fixed initial concentration of oxidant at 500 μM, as Fe^{2+} concentration was gradually increased from 0 to 500 μM ($[TPhP]_0/[oxidant]_0/[Fe^{2+}]_0$ = 1/50/0–1/50/50), TPhP degradation efficiency was improved correspondingly. TPhP degradation reached equilibrium quickly within 5 min reaction by Fenton process, while the degradation was increased gradually by PS process. As shown in Eqs. ((3), (6)), because the generated HO· would be quenched by the excessive Fe^{2+} and H_2O_2, TPhP degradation by Fenton oxidation was not increased with prolonging reaction time. When Fe^{2+} dosage was 50 μM ($[TPhP]_0/[oxidant]_0/[Fe^{2+}]_0$ = 1/50/5), TPhP degradation efficiency at 5 min was similar in both oxidation processes. When Fe^{2+} dosage was lower than 100 μM ($[TPhP]_0/[oxidant]_0/[Fe^{2+}]_0$ = 1/50/10), Fe^{2+}/PS process was more efficient than the

Fenton process for TPhP degradation. For example, as shown in Table S2, after 60 min, TPhP removal was 10.4%, 11.3%, 30.9%, and 45.3% by Fenton process, while it was 47.4%, 49.9%, 54.6%, and 67.9% by Fe^{2+}/PS process with Fe^{2+} concentrations of 5, 10, 50, and 100 μM, respectively. More efficient degradation of TPhP by Fe^{2+}/PS processmight because the generated $SO_4\cdot^-$ was more stable and selective than HO· [15,24]. In addition, Fe^{2+} could be transformed into Fe^{3+}, the production rate of HO· was thus greatly decreased in Fenton process, and hence TPhP degradation was reduced [12].

However, when Fe^{2+} concentration was increased to 500 μM ($[TPhP]_0/[oxidant]_0/[Fe^{2+}]_0$ = 1/50/50), 90.8% TPhP was degraded in 5 min by Fenton process, while only 72.4% TPhP was removed after 60 min by Fe^{2+}/PS process. This phenomenon may be because that 500 μM Fe^{2+} was sufficient to initiate adequate HO· to oxidize 10 μM TPhP in short reaction time. Results in Fig. 1a and b also indicated that HO· produced in Fenton process could be immediately consumed by TPhP and its degradation intermediates, while $SO_4\cdot^-$ was more stable because it selectively reacts with TPhP through the electron transfer mechanism [15,24]. In addition, as shown in Eq. (8), the excess Fe^{2+} in the solutions could scavenge $SO_4\cdot^-$, resulting in the inhibition on the oxidation of TPhP. Fe^{2+} in Fenton process can be regenerated in accordance with Eq. (2) and released into the next reaction cycle, while it was finally transformed to Fe^{3+} through Eqs. (7) and (8) and hence terminated the activation reaction in Fe^{2+}/PS process [12].

3.1.2. Effect of the initial oxidant dosage

As presented in Fig. 1c and d, the oxidation of TPhP by Fenton and Fe^{2+}/PS processes was further evaluated at different initial oxidant (i.e., H_2O_2 and PS) dosages (i.e., $[TPhP]_0/[Fe^{2+}]_0/[oxidant]_0$ = 1/50/0–1/50/100). Clearly, TPhP concentration in reaction solutions was not obviously changed by sole Fe^{2+} at 500 μM, while the obvious removal of TPhP by Fenton and Fe^{2+}/PS processes was observed. The degradation efficiency of TPhP after 60 min increased from 19.2% to 91.7% and from 12.4% to 84.1% by Fenton and Fe^{2+}/PS process with increasing initial ratio of $[TPhP]_0/[Fe^{2+}]_0/[oxidant]_0$ from 1/50/1 to 1/50/100, respectively. It should be noted that the difference of degradation efficiencies of TPhP by Fenton process with H_2O_2 concentrations at 500 and 1000 μM (i.e., $[TPhP]_0/[Fe^{2+}]_0/[oxidant]_0$ = 1/50/50 and 1/50/100) was little, 90.8% and 91.7%, respectively, which may be due to the limitation of Fe^{2+} concentration (Eq. (1)). As shown in Table S3, by Fe^{2+}/PS process, TPhP degradation efficiencies after 60 min was 12.3%, 28.9%, 72.4%, and 84.1% with the initial ratios of $[TPhP]_0/[Fe^{2+}]_0/[oxidant]_0$ as 1/50/1, 1/50/10, 1/50/50, and 1/50/100, respectively. Therefore, high amount of oxidants is required to achieve a better removal of TPhP in short time. Previous studies also found that in order to achieve higher removal efficiencies of pollutants, tens or hundreds times higher amount of oxidants is required [38,47,48]. Clearly, as PS concentration increased from 500 to 1000 μM, TPhP degradation efficiencies were similar (ca. 50%) after 5 min, and it was only enhanced to ca. 12% after 60 min reaction. This phenomenon could be caused by self-quenching of $SO_4\cdot^-$ radical by excessive PS to form less reactive $S_2O_8\cdot^-$ radical (Eq. (9)). In addition, the Fenton process was more efficient than Fe^{2+}/PS process for TPhP degradation with various initial oxidant dosages, implying that TPhP might be favorably degraded by HO· radical [15]. In both oxidation processes, taking into consideration both of proper removal efficiencies and cost saving, the optimal ratio of $[TPhP]_0/[Fe^{2+}]_0/[oxidant]_0$ was 1/50/50.

3.1.3. Effect of pH

It is well known that pH plays an important role in Fe^{2+}-activated ISCO applications [49]. Therefore, the effect of the initial solution pH ($pH_{initial}$) from 4.0 to 9.0 (typical pH of most natural waters [50,51]) on the degradation of TPhP by Fenton and Fe^{2+}/PS processes was evaluated and the degradation kinetics were presented in Fig. S1a and b. Fig. 2a and Table S4 summarized the degradation efficiency of TPhP after 60 min treatment. As $pH_{initial}$ increased from 4.0 to 9.0, the degradation efficiency of TPhP was slightly decreased from 93.0% to 86.8% by Fenton process, while it was almost no change in Fe^{2+}/PS process. The slight decrease of TPhP removal in Fenton process might be due to the precipitation of Fe^{2+} at high pHs. However, since $SO_4\cdot^-$ can react with OH^- to generate HO· under basic pH in Fe^{2+}/PS process (Eq. (12)) [45] with a high redox potential, TPhP could be efficiently degraded under a wide range of pH values. This observation was in agreement with previous studies regarding the degradation of organic contaminants by activated PS process [52,53]. It should be mentioned that all of the solution pHs (4.0–9.0) dropped to 3.2–3.8 after 60 min reaction, which might be due to the hydrolysis of ferrous ions, acidity of oxidant and its decomposition products (e.g., SO_4^{2-}), as well as the generation of acidic degradation by-products of TPhP [12]. The acidic pH greatly reduced Fe^{2+} precipitation and ensured its sufficient presence in the catalyzed oxidation. Furthermore, the outstanding performance of TPhP removal at wide pHs implied that Fenton and Fe^{2+}/PS processes based ISCO technology exhibited high application potential for remediating TPhP-contaminated waters.

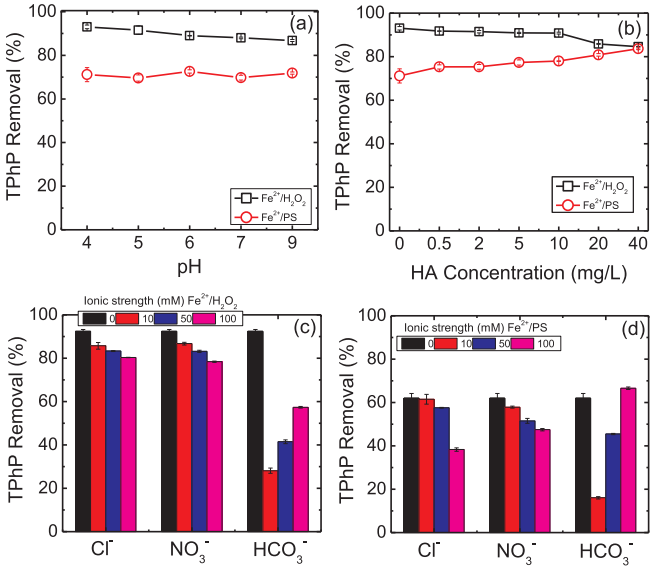

Fig. 2. Effect of (a) pH, (b) humic acid (HA), (c) and (d) anions on the removal of TPhP by Fenton process and Fe^{2+}/PS process. Experimental conditions: $[TPhP]_0$ = 10 μM, T = 25 °C, $[H_2O_2]_0$ = $[PS]_0$ = 500 μM, $[Fe^{2+}]_0$ = 500 μM, reaction time = 60 min, $pH_{initial}$ in (a) was adjusted by 0.1 M NaOH or HCl, and $pH_{initial}$ in (b), (c), (d) is 4.0. Errors represent the standard deviation (n = 3).

Acidic pH: $S_2O_8^{2-} + H^+ \rightarrow HS_2O_8^-$ (10)

$HS_2O_8^- + e^- \rightarrow SO_4^{\cdot-} + SO_4^{2-} + H^+$ (11)

Basic pH: $SO_4^{\cdot-} + HO^- \rightarrow +SO_4^{2-}$ (12)

3.1.4. Effect of HA

Natural organic matter (NOM) is ubiquitously present in natural waters, and can potentially influence the degradation of organic contaminants through AOPs [43–45]. Therefore, humic acid (HA, 0–40 mg/L), as a representative of aquatic NOM, was used to examine its influence on TPhP degradation in this study. TPhP degradation kinetics were presented in Fig. S1c and d. Fig. 2b, summarizing the degradation efficiencies of TPhP after 60 min treatment. As shown in Fig. 2b, TPhP removal efficiency dropped as HA concentration was increased in Fenton process, which was consistent with the findings in previous studies [54,55]. It has been considered that HA can serve as radical quenchers and can convert the radical intermediates to parent compounds [56]. In addition, HA can react with the HO· which was

produced in Fenton reaction [55]. Therefore, TPhP degradation efficiency was reduced due to the competition for HO· by HA.

On the contrary, in Fe^{2+}/PS process, the degradation of TPhP was promoted by HA, and TPhP removal increased from 71.2% to 83.6% with increasing HA concentration from 0 to 40 mg/L. HA can react with $SO_4\cdot^-$ and HO·, because the presence of electron-rich moieties e.g., carboxyl and hydroxyl functional groups [57]. Our previous study also demonstrated that HA possesses high reactivity towards $SO_4\cdot^-$ and HO· [45]. More radicals could be formed during HA oxidation in Fe^{2+}/PS process [58] and promoted the degradation of TPhP. In addition, semiquinone radicals, generated from hydroquinones, quinones, and phenols in HA, could also stimulate the decomposition of PS into $SO_4\cdot^-$ and HO· [59], resulting in the enhanced degradation of TPhP.

3.1.5. Effect of anions

In natural waters, the inorganic anions may have potential influence AOPs [43,44]. Therefore, in this study, the effect of the representative inorganic anions (i.e., Cl^-, NO_3^-, and HCO_3^-) at the concentration of 10, 50, and 100 mM on the degradation of TPhP via Fenton and Fe^{2+}/PS processes was evaluated, respectively, and the results were presented in Fig. 2c and d. As shown in Fig. 2c, all three examined anions at 10–100 mM inhibited degradation of TPhP in Fenton process, and the inhibition effects were different for these anions. With the presence of 10, 50, and 100 mM Cl^- and NO_3^-, TPhP removal efficiencies in Fenton process at 60 min were reduced from 92.4% to 85.7%, 83.3%, and 80.3% for Cl^-, and reduced to 86.7%, 83.2%, and 78.4% for NO_3, respectively However, the inhibition effect of HCO_3^- was alleviated with increasing HCO_3^- concentration. TPhP removal efficiencies in Fenton reaction were 28.1%, 41.5%, and 57.4% with the presence of 10, 50, and 100 mM HCO_3^-, respectively Similarly, the inhibition effects of Cl^- and NO_3^- on TPhP degradation were also observed in Fe^{2+}/PS process, indicating the inhibition increased with increasing concentration of Cl^- and NO_3^-. As shown in Fig. 2d, with the presence of 10, 50, and 100 mM Cl^- and NO_3^-, TPhP removal efficiencies in Fe^{2+}/PS process at 60 min were reduced from 62.0% to 61.5%, 57.6%, and 38.3% for Cl^-, and to 57.8%, 51.5%, and 47.5% for NO_3^-, respectively. 10 and 50 mM HCO_3^- suppressed TPhP degradation in Fe^{2+}/PS process with the removal efficiency of 16.1% and 45.5%, while 100 mM HCO_3^- enhanced TPhP degradation to 66.6%.

As reported, Cl^- can react with HO· [58] and SO4·$^-$ [60] to produce reactive chlorine radicals (including Cl·, $Cl_2\cdot^-$, HClOH·, and ClOH·$^-$) and free chlorine (e.g., Cl_2, HOCl, and OCl^-). Similarly, NO_3^- can react with HO· and SO4·$^-$ to generate $NO_2\cdot$ and $NO_3\cdot$ [58]. Because of these generated radicals exhibited relative weaker activity than SO4·$^-$ and HO· [61], the presence of Cl^- and NO_3^- could reduce the degradation efficiency of TPhP in Fenton and Fe^{2+}/PS processes. Similar results have also been reported in previous studies [62,63]. In addition, the inhibition effects of Cl^- and NO_3^- in Fenton process were lower than that in Fe^{2+}/PS process, which could be due to the higher reactive ability of HO· than $SO_4\cdot^-$ towards these anions [58,64].

However, the inhibition effect of HCO_3^- on TPhP degradation was different compared to Cl^- and NO_3^-, which was inversely related to HCO_3^- concentration. Specifically, TPhP removal efficiencies at 60 min with the presence of 10, 50, and 100 mM HCO_3^- were 28.1%, 47.5%, and 57.4% in Fenton process, and were 16.1%, 45.5%, and 66.6% in Fe^{2+}/PS process, respectively. The promotion effect was also observed with the addition of 100 mM HCO_3^- in Fe^{2+}/PS process. Table S5 showed that the addition of 10–100 mM HCO_3^- adjusted the solution pH from 4.0 to 7.4–8.7. It is well known that ferrous ions tend to co-precipitate when the pH is > 3, and hence would weaken the ferrous ion-activated oxidation [15]. Furthermore, HCO_3^- was demonstrated to be an efficient scavenger for $SO_4\cdot^-$ and HO· and thus produced less reactive carbonate radicals ($HCO_3\cdot$ and $CO_3\cdot^-$) [43,52,56]. Therefore, the presence of HCO_3^- significantly reduced the removal efficiency of TPhP. Although the carbonate radicals are less reactive than $SO_4\cdot^-$ and HO·, it can favorably react with the electron-rich moieties at a fairly high rate [47]. Similarly, TPhP, as an electron-rich chemical [41], might favorably react with carbonate radicals and hence enhanced TPhP removal efficiency with the increasing concentration of HCO_3^-. Previous study also found that the presence of HCO_3^- could promote the degradation of sulfamethoxazole by thermo activated PS, probably because of the electron-rich aniline moieties present in sulfamethoxazole structure [47]. Moreover, HCO_3^- at high concentration could stimulate the decomposition of PS and H_2O_2 into $SO_4\cdot^-$ and HO·, respectively, [59,65] and hence promoted the degradation of TPhP.

3.2. Identification of dominating reactive radicals

Radical quenching experiments were conducted at pH 4.0 to identify radicals contributing to the oxidation of TPhP by Fenton and Fe^{2+}/PS processes. As suggested, EtOH containing α-hydrogen reacts with $SO_4\cdot^-$ at $1.6–7.7 \times 10^7\ M^{-1}s^{-1}$ and with HO· at $1.2–2.8 \times 10^9\ M^{-1}s^{-1}$, respectively, while the reaction rate of TBA (without the α-hydrogen) with HO· ($k_{HO\cdot} = 3.8–7.6 \times 10^8\ M^{-1}s^{-1}$) is much higher than that with $SO_4\cdot^-$ ($k_{SO4\cdot^-} = 4–9.1 \times 10^5\ M^{-1}s^{-1}$) [15,45]. Therefore, EtOH can be used to scavenge both $SO_4\cdot^-$ and HO· radicals, whereas TBA can be applied to quench HO· [19,47]. In this study, EtOH and TBA were used as the radical scavengers to identify the dominant reactive radicals ($SO_4\cdot^-$ and HO·) for TPhP degradation in Fenton and Fe^{2+}/PS processes, and the results were presented in Fig. 3. For Fenton system, the degradation efficiency of TPhP at 60 min was 92% without the presence of radical quenchers, while it was greatly reduced to 27% and 13% with the addition of 12.5 mM TBA or EtOH, respectively (Fig. 3a). Both TBA and EtOH greatly inhibited TPhP degradation by Fenton process, indicating that HO· was the main radical in TPhP degradation in Fenton reaction. In Fe^{2+}/PS process, on the other side, the degradation efficiency of TPhP at 60 min was reduced to 72% without any radical quenchers, while TPhP degradation efficiencies dropped to 54% and 30% with the addition of 12.5 mM TBA or EtOH, respectively (Fig. 3b). The results indicated that both $SO_4\cdot^-$ and HO· radicals could contribute to the oxidation of TPhP in Fe^{2+}/PS process. Meanwhile, TBA showed less inhibition effect than EtOH due to its slow reaction with $SO_4\cdot^-$, implying that $SO_4\cdot^-$ could be the predominant species for TPhP degradation in Fe^{2+}/PS process at pH 4. Furthermore, the effects of HO· and $SO_4\cdot^-$ on the degradation of TPhP

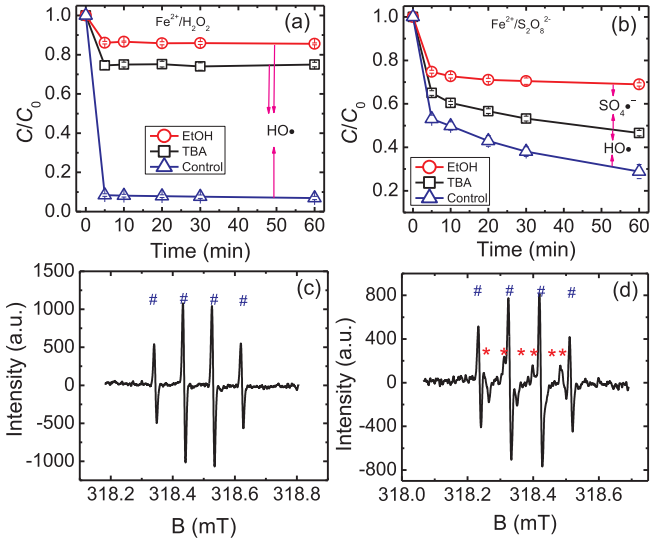

Fig. 3. Kinetics of TPhP degradation in the presence of the radical quenchers EtOH and TBA by (a) Fenton and (b) Fe^{2+}/PS process; EPR spectra of hydroxyl and sulfate radicals trapped by DMPO in the (c) Fenton and (d) Fe^{2+}/PS process (#: HO·, and *: $SO_4\cdot^-$). Experimental conditions: $[TPhP]_0 = 10\ \mu M$, $pH_{initial} = 4.0$, $T = 25\ ^\circ C$, $[H_2O_2]_0 = [PS]_0 = 500\ \mu M$, $[Fe^{2+}]_0 = 500\ \mu M$. Errors represent the standard deviation (n = 3).

were quantified and listed in Table S6. In Fenton process, the contribution of HO· was calculated to be 84.5% based on EtOH quenching result. While in Fe^{2+}/PS process, the contributions of HO· and SO_4·$^-$ were 24.9% and 31.4%, respectively. However, although EtOH could quench HO· and SO_4·$^-$ radicals, TPhP were still degraded in the presence of EtOH in both processes, indicating that other process (e.g., coagulation) or other radical species (e.g., HO_2·, O_2·$^-$, S_2O_8·$^-$) could possibly contribute to the TPhP degradation [66].

EPR was further employed to detect the active species produced from Fenton and Fe^{2+}/PS processes *in situ*. As shown in Fig. 3c and d, HO· was captured by DMPO in the Fenton reaction, while both HO· and SO_4·$^-$ were captured in the Fe^{2+}/PS system. Moreover, the radical intensity of Fenton reaction is higher than that of Fe^{2+}/PS process, which results in fast degradation of TPhP in Fenton reaction.

3.3. Degradation products and pathways

The degradation products of TPhP via Fenton and Fe^{2+}/PS oxidation were identified by LC-MS/MS analysis which was operated at the positive ionization mode ($[M+H]^+$). Fig. S2a and b showed the total ion chromatograms (TICs) of TPhP and its degradation products by Fenton and Fe^{2+}/PS oxidation, respectively. No product was detected in the control group which contained no oxidants. In addition to TPhP (retention time = 1.91 min), 4 intermediate products were observed at elution time of 0.60, 0.82, 1.08, and 1.32 min in Fenton reaction (Fig. S2a), while 3 main degradation products were observed at 0.59, 1.06, and 1.31 min in Fe^{2+}/PS oxidation (Fig. S2b), respectively. For Fenton process, the 4 products showed molecular peaks with *m/z* values of 267.2 (P2), 359.3 (P4), 343.3 (P3), and 251.2 (P1), respectively. For Fe^{2+}/PS process, the 3 products displayed the peaks with *m/z* values of 267.0 (P2), 343.3 (P3), and 251.2(P1), respectively. Because products P1-3 showed similar retention time and *m/z* values in both processes, it was considered that same products P1-3 were generated during TPhP degradation in both Fenton and Fe^{2+}/PS oxidation processes. Further MS/MS analysis was performed to elucidate the possible molecular structures for the degradation products (Fig. S3).

Peaks of *m/z* 251 (P1), 267 (P2), 343 (P3), and 359 (P4) were individually assigned as diphenyl phosphate (Fig. S3a), OH-diphenyl phosphate (Fig. S3b), OH-triphenyl phosphate (Fig. S3c), and di-OH-triphenyl phosphate (Fig. S3d). Furthermore, the degradation pathways of TPhP via Fenton and Fe^{2+}/PS oxidation were proposed based on product identification and HO·/SO_4·$^-$ radical oxidation mechanisms (Fig. 4). Generally, HO· can react with pollutants through hydrogen abstraction, direct addition, or electron-transfer, resulting in the formation of different products [67], while SO_4·$^-$ mainly reacted with chemicals through electron-transfer mechanism, generating the adduct intermediates or radical cations [68]. The generating pathway of product P1 (*m/z* 251, Fig. S3a) could involve a two-step reaction (Fig. 4a and c). At first, a HO· was added on the phosphoric center [32], then a cleavage of one phenoxy bond occurred to form product P1. HO· could further attack the phenyl group on P1 and generated product P2 (*m/z* 267, Fig. 4a). Through Fe^{2+}/PS oxidation, the benzene ring of P1 could be attacked by SO_4·$^-$, generating a cation radical [36,47], then the cation radical reacted with water to form product P2 (*m/z* 267, Fig. 4c). In Fenton reaction, product P3 (*m/z* 343, Fig. 4b) was formed through direct addition of OH to phenyl group on TPhP, and further OH addition on P3 generated product P4 (*m/z* 359). By Fe^{2+}/PS oxidation, product P3 (*m/z* 343, Fig. 4d) could be formed by the attack of SO_4·$^-$ to phenyl group on TPhP to form a cation radical, followed by reacting with water. It should be noted that although TOC reduction via TPhP degradation in both Fenton and Fe^{2+}/PS oxidation processes was observed, almost no PO_4^{3-} was detected (Fig. S5), indicating that the generated products (P1-4) could be refractory to be degraded compared to TPhP. Similarly, Xu et al. [38] suggested that hydroxylation and C-O bond cleavage were mainly involved in the degradation pathways of TCEP by UV/PMS where HO· and SO_4·$^-$ were identified as dominant radicals. They also considered that C—O bond was the favorable reaction site than P=O double bond, which might be the reason why no PO_4^{3-} was detected in this study.

3.4. Degradation of TPhP in natural waters

In order to evaluate the technical feasibility of ferrous ion-activated hydrogen peroxide and persulfate oxidation for TPhP removal from natural waters, the degradation efficiencies of TPhP in different natural water matrices (Table S1, Supplementary Data) were examined. The pHs of four collected water samples (Municipal effluent, Zhujiang River water, South China Sea water, and tap water) were in the range of 7.03–8.33. Because TPhP removal would not be obviously influenced by solution pH values (Fig. 2a), DI water at pH 7.0 was prepared for better understanding the effect of water constituents. The experiments were conducted at the $[TPhP]_0/[Fe^{2+}]_0/[oxidant]_{0\,M}$ ratio of 1/50/50,

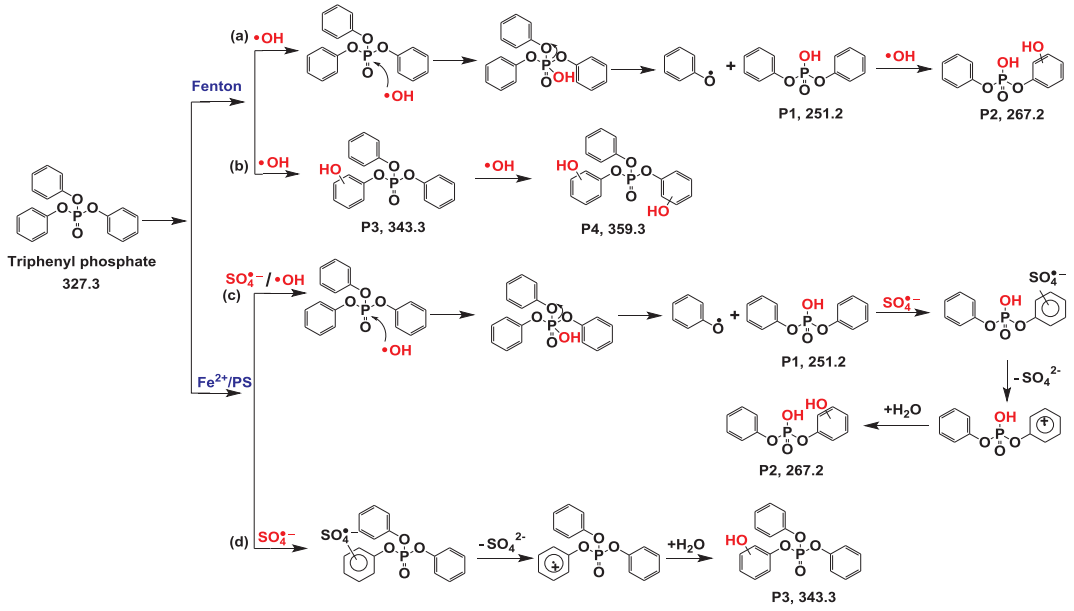

Fig. 4. Possible degradation products and the proposed transformation pathways of TPhP via Fenton and Fe^{2+}/PS oxidation.

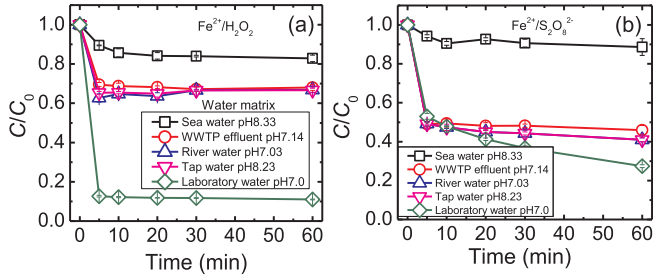

Fig. 5. Degradation of TPhP by (a) Fenton system and (b) PS system in different water matrices. Experimental conditions: $[TPhP]_0$ = 10 μM, T = 25 °C, $[H_2O_2]_0$ = $[PS]_0$ = 500 μM, $[Fe^{2+}]_0$ = 500 μM, and reaction time = 60 min. Errors represent the standard deviation (n = 3).

and the results were presented in Fig. 5. Obviously, TPhP degradation was inhibited in all natural waters than that in PBS buffer, with the lowest value in sea water following with municipal effluent water, river water and then tap water. For example, after 60 min, Fenton process was able to remove 89.0%, 33.3%, 33.2%, 32.0%, and 17.2% of TPhP, and Fe^{2+}/PS process could remove 72.7%, 59.1%, 59.0%, 54.1%, and 11.4% of TPhP from PBS buffer, tap water, river water, municipal effluent, and sea water, respectively. As discussed previously, the various constituents, including NOM and anions that are present in natural water matrices (Table S1), could contribute significantly to the inhibitory effect. In particular, TPhP degradation was greatly inhibited in seawater matrix. As shown in Table S1, the high concentration of Cl^- (> 18000 mg/L) was detected in the collected seawater. This may be the main reason to explain the low removal of TPhP in sea water compared to that in the other three types of waters. Because Cl^- in seawater at high concentration could react with HO· and SO_4·$^-$ radicals to compete with target compounds and generate weaker radicals, which inhibited the TPhP degradation. The results here indicated that higher oxidant dosage and longer reaction time were necessary for the complete removal of TPhP from natural waters [45,48]. Nevertheless, the discharge permission needs to be considered when the oxidant dosage is increased. For example, according to Environmental Quality Standard for Surface Water of China (GB 3838–2002), the upper limit concentration of sulfate ion in surface water is 250 mg L^{-1}. In this study, the maximum dosage of PS used is ca. 86 mg L^{-1} sulfate ion, which is lower than the value specified in Standard and thus will be permissible to be discharged.

4. Conclusions

This study evaluated the degradation of TPhP under different experimental conditions in Fenton and Fe^{2+}/PS processes. Results showed that both Fenton and Fe^{2+}/PS processes are efficient techniques for removing of TPhP from aqueous solution. The main conclusions are as follows:

(1). At the condition of $[TPhP]_0/[Fe^{2+}]_0/[oxidant]_0$ = 1/50/50, 25 °C at pH 4.0, removal efficiencies of 10 μM TPhP were 90.8% after 5 min treatment by Fenton process and 72.4% after 60 min treatment by Fe^{2+}/PS process, respectively.
(2). High removal of TPhP can be achieved under a wide range of pH (4.0–9.0) in both processes.
(3). EPR experiments showed that with the same Fe^{2+} and oxidants dosage, the HO· generated in Fenton process exhibited higher intensity than HO· and SO_4·$^-$ generated in Fe^{2+}/PS process, resulting in a high removal of TPhP in short time.
(4). Products identification showed that the TPhP degradation products were similar in both oxidation processes, and the degradation pathways included hydroxylation and phenoxy bond cleavage.
(5). Nature water constituents, HA, Cl^-, and NO_3^-, exhibited no obvious influence on TPhP degradation, while HCO_3^- significantly inhibited TPhP oxidation with an inversed relationship with HCO_3^- concentration. High oxidant dosage and long oxidation time were required to achieve high removal efficiencies and more complete mineralization of TPhP from natural waters.

Acknowledgments

This work was supported by the National Natural Science Foundation of China (21707019), the Science and Technology Planning Project of Guangzhou City (201804010396), the Characteristic Innovation Project of High Education Department of Guangdong Province (2017KTSCX058), and the Science and Technology Planning Project of Guangdong Province (2017A050506052, 2017A020216010, and 2017B020216003).

Appendix A. Supplementary data

Supplementary data to this article can be found online at https://doi.org/10.1016/j.cej.2018.12.140.

References

[1] I. van der Veen, J. de Boer, Phosphorus flame retardants: Properties, production, environmental occurrence, toxicity and analysis, Chemosphere 88 (2012) 1119–1153.
[2] H.M. Stapleton, S. Klosterhaus, S. Eagle, J. Fuh, J.D. Meeker, A. Blum, T.F. Webster, Detection of organophosphate flame retardants in furniture foam and US house dust, Environ. Sci. Technol. 43 (2009) 7490–7495.
[3] R. Wang, J. Tang, Z. Xie, W. Mi, Y. Chen, H. Wolschke, C. Tian, X. Pan, Y. Luo, R. Ebinghaus, Occurrence and spatial distribution of organophosphate ester flame retardants and plasticizers in 40 rivers draining into the Bohai Sea, north China, Environ. Pollut. 198 (2015) 172–178.
[4] S. Cao, X. Zeng, H. Song, H. Li, Z. Yu, G. Sheng, J. Fu, Levels and distributions of organophosphate flame retardants and plasticizers in sediment from Taihu Lake China, Environ. Toxicol. Chem. 31 (2012) 1478–1484.
[5] A.M. Sundkvist, U. Olofsson, P. Haglund, Organophosphorus flame retardants and plasticizers in marine and fresh water biota and in human milk, J. Environ. Monit. 12 (2010) 943–951.
[6] H. Carlsson, U. Nilsson, C. Ostman, Video display units: an emission source of the contact allergenic flame retardant triphenyl phosphate in the indoor environment, Environ. Sci. Technol. 34 (2000) 3885–3889.
[7] G. Su, D. Crump, R.J. Letcher, S.W. Kennedy, Rapid in vitro metabolism of the flame retardant triphenyl phosphate and effects on cytotoxicity and mRNA expression in chicken embryonic hepatocytes, Environ. Sci. Technol. 48 (2014) 13511–13519.
[8] Q. Shi, M. Wang, F. Shi, L. Yang, Y. Guo, C. Feng, J. Liu, B. Zhou, Developmental neurotoxicity of triphenyl phosphate in zebrafish larvae, Aquat. Toxicol. (2018).
[9] M.M. Huber, S. Canonica, G.Y. Park, U. Von Gunten, Oxidation of pharmaceuticals during ozonation and advanced oxidation processes, Environ. Sci. Technol. 37 (2003) 1016–1024.
[10] M. Klavarioti, D. Mantzavinos, D. Kassinos, Removal of residual pharmaceuticals from aqueous systems by advanced oxidation processes, Environ. Int. 35 (2009) 402–417.
[11] R.C. Zhang, P.Z. Sun, T.H. Boyer, L. Zhao, C.H. Huang, Degradation of pharmaceuticals and metabolite in synthetic human urine by UV, UV/H_2O_2, and UV/PDS, Environ. Sci. Technol. 49 (2015) 3056–3066.
[12] I. Epold, M. Trapido, N. Dulova, Degradation of levofloxacin in aqueous solutions by Fenton, ferrous ion-activated persulfate and combined Fenton/persulfate systems, Chem. Eng. J. 279 (2015) 452–462.
[13] S. Wang, A Comparative study of Fenton and Fenton-like reaction kinetics in decolourisation of wastewater, Dyes Pigm. 76 (2008) 714–720.
[14] H. Lee, M. Shoda, Removal of COD and color from livestock wastewater by the Fenton method, J. Hazard. Mater. 153 (2008) 1314–1319.
[15] N. Dulova, E. Kattel, M. Trapido, Degradation of naproxen by ferrous ion-activated hydrogen peroxide, persulfate and combined hydrogen peroxide/persulfate processes: The effect of citric acid addition, Chem. Eng. J. 318 (2017) 254–263.
[16] N. Yan, F. Liu, W. Huang, Interaction of oxidants in siderite catalyzed hydrogen peroxide and persulfate system using trichloroethylene as a target contaminant, Chem. Eng. J. 219 (2013) 149–154.
[17] R.L. Johnson, P.G. Tratnyek, R.O.B. Johnson, Persulfate persistence under thermal activation conditions, Environ. Sci. Technol. 42 (2008) 9350–9356.
[18] A. Ghauch, A. Baalbaki, M. Amasha, R. El Asmar, O. Tantawi, Contribution of persulfate in UV-254 nm activated systems for complete degradation of chloramphenicol antibiotic in water, Chem. Eng. J. 317 (2017) 1012–1025.
[19] G.P. Anipsitakis, D.D. Dionysiou, Radical generation by the interaction of transition metals with common oxidants, Environ. Sci. Technol. 38 (2004) 3705–3712.
[20] A. Ghauch, G. Ayoub, S. Naim, Degradation of sulfamethoxazole by persulfate assisted micrometric Fe-0 in aqueous solution, Chem. Eng. J. 228 (2013) 1168–1181.
[21] G. Ayoub, A. Ghauch, Assessment of bimetallic and trimetallic iron-based systems

for persulfate activation: application to sulfamethoxazole degradation, Chem. Eng. J. 256 (2014) 280–292.
[22] S. Naim, A. Ghauch, Ranitidine abatement in chemically activated persulfate systems: assessment of industrial iron waste for sustainable applications, Chem. Eng. J. 288 (2016) 276–288.
[23] X.G. Duan, H.Q. Sun, J. Kang, Y.X. Wang, S. Indrawirawan, S.B. Wang, Insights into heterogeneous catalysis of persulfate activation on dimensional-structured nanocarbons, ACS Catal. 5 (2015) 4629–4636.
[24] P. Neta, V. Madhavan, H. Zemel, R.W. Fessenden, Rate constants and mechanism of reaction of sulfate radical anion with aromatic compounds, J. Am. Chem. Soc. 99 (1977) 163–164.
[25] H.V. Lutze, S. Bircher, I. Rapp, N. Kerlin, R. Bakkour, M. Geisler, C. von Sonntag, T.C. Schmidt, Degradation of chlorotriazine pesticides by sulfate radicals and the influence of organic matter, Environ. Sci. Technol. 49 (2015) 1673–1680.
[26] A. Ghauch, A. Tuqan, Oxidation of bisoprolol in heated persulfate/H_2O systems: kinetics and products, Chem. Eng. J. 183 (2012) 162–171.
[27] G. Zhen, X. Lu, L. Su, T. Kobayashi, G. Kumar, T. Zhou, K. Xu, Y.Y. Li, X. Zhu, Y. Zhao, Unraveling the catalyzing behaviors of different iron species (Fe^{2+} vs. Fe (0)) in activating persulfate-based oxidation process with implications to waste activated sludge dewaterability, Water Res. 134 (2018) 101–114.
[28] B. Liu, F. Qu, W. Chen, H. Liang, T. Wang, X. Cheng, H. Yu, G. Li, B. Van der Bruggen, Microcystis aeruginosa-laden water treatment using enhanced coagulation by persulfate/Fe(II), ozone and permanganate: Comparison of the simultaneous and successive oxidant dosing strategy, Water Res. 125 (2017) 72–80.
[29] M. Antonopoulou, A. Giannakas, F. Bairamis, M. Papadaki, I. Konstantinou, Degradation of organophosphorus flame retardant tris (1-chloro-2-propyl) phosphate (TCPP) by visible light N, S-codoped Ti_O2 photocatalysts, Chem. Eng. J. 318 (2017) 231–239.
[30] T. Tang, G.N. Lu, W.J. Wang, R. Wang, K.B. Huang, Z.Y. Qiu, X.Q. Tao, Z. Dang, Photocatalytic removal of organic phosphate esters by TiO_2: Effect of inorganic ions and humic acid, Chemosphere 206 (2018) 26–32.
[31] M. Antonopoulou, P. Karagianni, I. Konstantinou, Kinetic and mechanistic study of photocatalytic degradation of flame retardant Tris 1-chloro-2-propyl) phosphate (TCPP), Appl. Catal. B 192 (2016) 152–160.
[32] J.S. Ye, J. Liu, C.S. Li, P.L. Zhou, S. Wu, H.S. Ou, Heterogeneous photocatalysis of tris(2-chloroethyl) phosphate by UV/TiO_2: degradation products and impacts on bacterial proteome, Water Res. 124 (2017) 29–38.
[33] Y.J. Chen, J.S. Ye, Y. Chen, H. Hu, H.L. Zhang, H.S. Ou, Degradation kinetics, mechanism and toxicology of tris(2-chloroethyl) phosphate with 185 nm vacuum ultraviolet, Chem. Eng. J. 356 (2019) 98–106.
[34] X.C. Ruan, R. Ai, X. Jin, Q.F. Zeng, Z.Y. Yang, Photodegradation of tri (2-chloroethyl) phosphate in aqueous solution by UV/H_2O_2, Water Air Soil Pollut. 224 (2013).
[35] M.J. Watts, K.G. Linden, Photooxidation and subsequent biodegradability of recalcitrant tri-alkyl phosphates TCEP and TBP in water, Water Res. 42 (2008) 4949–4954.
[36] J. Liu, J.S. Ye, Y.F. Chen, C.S. Li, H.S. Ou, UV-driven hydroxyl radical oxidation of tris(2-chloroethyl) phosphate: Intermediate products and residual toxicity, Chemosphere 190 (2018) 225–233.
[37] X.C. Ruan, X. Jin, Z.Y. Yang, Q.F. Zeng, Photodegradation of tri(chloropropyl) phosphate solution by UV/O_3, Water Air Soil Pollut. 225 (2014).
[38] X. Xu, J. Chen, R. Qu, Z. Wang, Oxidation of Tris (2-chloroethyl) phosphate in aqueous solution by UV-activated peroxymonosulfate: kinetics, water matrix effects, degradation products and reaction pathways, Chemosphere 185 (2017) 833–843.
[39] H.S. Ou, J. Liu, J.S. Ye, L.L. Wang, N.Y. Gao, J. Ke, Degradation of tris(2-chloroethyl) phosphate by ultraviolet-persulfate: kinetics, pathway and intermediate impact on proteome of *Escherichia coli*, Chem. Eng. J. 308 (2017) 386–395.
[40] X.J. Yuan, S. Lacorte, J. Cristale, R.F. Dantas, C. Sans, S. Esplugas, Z.M. Qiang, Removal of organophosphate esters from municipal secondary effluent by ozone and UV/H_2O_2 treatments, Sep. Purif. Technol. 156 (2015) 1028–1034.
[41] Q. Yu, H.B. Xie, J.W. Chen, Atmospheric chemical reactions of alternatives of polybrominated diphenyl ethers initiated by •OH: a case study on triphenyl phosphate, Sci. Total Environ. 571 (2016) 1105–1114.
[42] C. Li, G.L. Wei, J.W. Chen, Y.H. Zhao, Y.N. Zhang, L.M. Su, W.C. Qin, Aqueous •OH radical reaction rate constants for organophosphorus flame retardants and plasticizers: Experimental and modeling studies, Environ. Sci. Technol. 52 (2018) 2790–2799.
[43] L.R. Bennedsen, J. Muff, E.G. Sogaard, Influence of chloride and carbonates on the reactivity of activated persulfate, Chemosphere 86 (2012) 1092–1097.
[44] J. Deng, Y.S. Shao, N.Y. Gao, Y. Deng, S.Q. Zhou, X.H. Hu, Thermally activated persulfate (TAP) oxidation of antiepileptic drug carbamazepine in water, Chem. Eng. J. 228 (2013) 765–771.
[45] Y. Feng, Q. Song, W. Lv, G. Liu, Degradation of ketoprofen by sulfate radical-based advanced oxidation processes: Kinetics, mechanisms, and effects of natural water matrices, Chemosphere 189 (2017) 643–651.
[46] Z.J. Xie, Y.P. Feng, F.L. Wang, D.N. Chen, Q.X. Zhang, Y.Q. Zeng, W.Y. Lv, G.G. Liu, Construction of carbon dots modified MoO_3/g-C_3N_4 Z-scheme photocatalyst with enhanced visible-light photocatalytic activity for the degradation of tetracycline, Appl. Catal. B 229 (2018) 96–104.
[47] Y.F. Ji, Y. Fan, K. Liu, D.Y. Kong, J.H. Lu, Thermo activated persulfate oxidation of antibiotic sulfamethoxazole and structurally related compounds, Water Res. 87 (2015) 1–9.
[48] A. Ghauch, A. Tuqan, N. Kibbi, Naproxen abatement by thermally activated persulfate in aqueous systems, Chem. Eng. J. 279 (2015) 861–873.
[49] T. Li, Z. Zhao, Q. Wang, P. Xie, J. Ma, Strongly enhanced Fenton degradation of organic pollutants by cysteine: an aliphatic amino acid accelerator outweighs hydroquinone analogues, Water Res. 105 (2016) 479–486.
[50] Y. Feng, X. Liu, K.A. Huynh, J.M. McCaffery, L. Mao, S. Gao, K.L. Chen, Heteroaggregation of graphene oxide with nanometer-and micrometer-sized hematite colloids: influence on nanohybrid aggregation and microparticle sedimentation, Environ. Sci. Technol. (2017).
[51] Y.P. Feng, K.A. Huynh, Z.J. Xie, G.G. Liu, S.X. Gao, Heteroaggregation and sedimentation of graphene oxide with hematite colloids: Influence of water constituents and impact on tetracycline adsorption, Sci. Total Environ. 647 (2019) 708–715.
[52] C.J. Liang, Z.S. Wang, N. Mohanty, Influences of carbonate and chloride ions on persulfate oxidation of trichloroethylene at 20 °C, Sci. Total Environ. 370 (2006) 271–277.
[53] E. Hayon, A. Treinin, J. Wilf, Electronic spectra, photochemistry, and autoxidation mechanism of the sulfite-bisulfite-pyrosulfite systems. SO_2^-, SO_3^-, SO_4^-, and SO_5^- radicals, J. Am. Chem. Soc. 94 (1972) 47–57.
[54] F. Wang, Y. Wu, Y. Gao, H. Li, Z. Chen, Effect of humic acid, oxalate and phosphate on Fenton-like oxidation of microcystin-LR by nanoscale zero-valent iron, Sep. Purif. Technol. 170 (2016) 337–343.
[55] A. Georgi, A. Schierz, U. Trommler, C.P. Horwitz, T.J. Collins, F.D. Kopinke, Humic acid modified Fenton reagent for enhancement of the working pH range, Appl. Catal. B 72 (2007) 26–36.
[56] Y. Fan, Y.F. Ji, D.Y. Kong, J.H. Lu, Q.S. Zhou, Kinetic and mechanistic investigations of the degradation of sulfamethazine in heat-activated persulfate oxidation process, J. Hazard. Mater. 300 (2015) 39–47.
[57] H.P. Gao, J.B. Chen, Y.L. Zhang, X.F. Zhou, Sulfate radicals induced degradation of triclosan in thermally activated persulfate system, Chem. Eng. J. 306 (2016) 522–530.
[58] C.Q. Tan, N.Y. Gao, Y. Deng, Y.J. Zhang, M.H. Sui, J. Deng, S.Q. Zhou, Degradation of antipyrine by UV, UV/H_2O_2 and UV/PS, J. Hazard. Mater. 260 (2013) 1008–1016.
[59] Y.H. Guan, J. Ma, Y.M. Ren, Y.L. Liu, J.Y. Xiao, L.Q. Lin, C. Zhang, Efficient degradation of atrazine by magnetic porous copper ferrite catalyzed peroxymonosulfate oxidation via the formation of hydroxyl and sulfate radicals, Water Res. 47 (2013) 5431–5438.
[60] Y. Yang, J.J. Pignatello, J. Ma, W.A. Mitch, Comparison of halide impacts on the efficiency of contaminant degradation by sulfate and hydroxyl radical-based advanced oxidation processes AOPs, Environ. Sci. Technol. 48 (2014) 2344–2351.
[61] R. Yuan, S.N. Ramjaun, Z. Wang, J. Liu, Effects of chloride ion on degradation of Acid Orange 7 by sulfate radical-based advanced oxidation process: implications for formation of chlorinated aromatic compounds, J. Hazard. Mater. 196 (2011) 173.
[62] C.-H. Liao, S.-F. Kang, F.-A. Wu, Hydroxyl radical scavenging role of chloride and bicarbonate ions in the H_2O_2/UV process, Chemosphere 44 (2001) 1193–1200.
[63] Y. Yang, J.J. Pignatello, J. Ma, W.A. Mitch, Effect of matrix components on UV/H_2O_2 and UV/$S_2O_8^{2-}$ advanced oxidation processes for trace organic degradation in reverse osmosis brines from municipal wastewater reuse facilities, Water Res. 89 (2016) 192–200.
[64] H.V. Lutze, N. Kerlin, T.C. Schmidt, Sulfate radical-based water treatment in presence of chloride: formation of chlorate, inter-conversion of sulfate radicals into hydroxyl radicals and influence of bicarbonate, Water Res. 72 (2015) 349–360.
[65] L. Zhao, Z. Sun, J. Ma, H. Liu, Influencing mechanism of bicarbonate on the catalytic ozonation of nitrobenzene in aqueous solution by ceramic honeycomb supported manganese, J. Mol. Catal. A: Chem. 322 (2010) 26–32.
[66] S. Akbari, F. Ghanbari, M. Moradi, Bisphenol A degradation in aqueous solutions by electrogenerated ferrous ion activated ozone, hydrogen peroxide and persulfate: Applying low current density for oxidation mechanism, Chem. Eng. J. 294 (2016) 298–307.
[67] R.C. Zhang, Y.K. Yang, C.H. Huang, N. Li, H. Liu, L. Zhao, P.Z. Sun, UV/H_2O_2 and UV/PDS treatment of trimethoprim and sulfamethoxazole in synthetic human urine: Transformation products and toxicity, Environ. Sci. Technol. 50 (2016) 2573–2583.
[68] L.W. Matzek, K.E. Carter, Activated persulfate for organic chemical degradation: A review, Chemosphere 151 (2016) 178–188.